Electrons Dynamics in Asymmetric Magnetic Reconnection and Rapid Island Coalescence: Anisotropy and Agyrotropy With and Without a Guide Field

E. Cazzola[1], M. E. Innocenti[1], M. V. Goldman[2], D. L. Newman[2], S. Markidis[3], G. Lapenta[1]

[1] *CmPA, Department of Mathematics, KULeuven University, Leuven, Belgium*

[2] *Center for Integrated Plasma Studies, University of Colorado Boulder, Boulder (CO), USA*

[3] *PDC Center for high Performance Computing, KTH, Stockholm, Sweden*

This work intends to give further support to the recently launched NASA MultiScale Magnetospheric Mission (MMS) on the electron anisotopy and agyrotropy, throughout resolved kinetic simulations of asymmetric magnetic reconnection at the magnetopause.

Two different reconnection configurations are addressed. The first configuration represents the typical single X-point reconnection evolution, as found in the literature (e.g. [4]). The second configuration is instead set in order to better analyze the physics of magnetic island coalescence in asymmetric conditions. In a previous work, three different reconnection regions have been identified in the case without guide field ([1]), marked as X-, D- and M-regions, which are further studied here for the case with guide field. We compare results from different numerical algorithms designed to render the non-gyrotropy from Particle-in-Cell (PIC) simulations. Two robust algorithms are considered, such as those proposed in [5] and [6]. A third metric is also adopted based on the local magnetic field frame of reference, following what proposed in [2]. Finally, in light of the upcoming satellite data from MMS, a set of different electron velocity distributions are additionally given for some specific regions to help distinguish them from upcoming observations.

Results and Conclusion. Simulations are performed using the Fully Kinetic Implicit Moment Particle-in-Cell code iPIC3D [3]. Figures 2 and 3 show, respectively, the outcomes from the algorithms mentioned earlier and the phase-space (PS) taken in some relevant regions marked with a black box in Figure 2. A new velocity representation is adopted for the phase-spaces, as defined in Figure 1. Additionally, Table 1 gives a summary of the principal features found in the analysis. In the case without guide

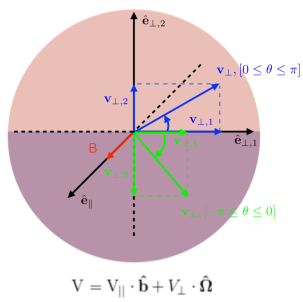

Figure 1: *Definition of $V_{\perp}$ and θ.*

Table 1: *Summary table comparing the results from all the algorithms analyzed.*

Without Guide Field						
Region	$T_{\parallel}/\mathbf{T}_{\perp_1}$	$T_{\perp_1}/\mathbf{T}_{\perp_2}$	**AO**	$\sqrt{\mathbf{Q}}$	$\mathbf{V}_{\parallel}-\mathbf{V}_{\perp}$	$\theta-\mathbf{V}_{\perp}$
Method Features	Frame-dependent Useful for quick assessments Qualitative results Results similar to both *AO* and $\sqrt{Q}$		Quantitative results *AO* computed in the plane, $\sqrt{Q}$ computed 3D Strong agreement between the methods		Direct Comparison with Satellite observations Direct and Clear Assessment of anisotropy and agyrotropy	
Region X (Domain 1)	Medium	Remarked	15%	$10-15\%$	low	Remarked Crescent-shape distribution on $V_{\perp_1}-V_{\perp_2}$ plane
Region D (Domain 2)	Remarked	Remarked	15%	15%	Remarked double beam flat top distribution	Remarked
Region M (Domain 3)	Not-detected	Not-detected	Not-detected	Not-detected	Low	Not-Detected
Separatrices (Domains 5 and 7)	Medium	Not-detected	15%	$10-15\%$	Relevant for slow electrons	Low
Magnetic Island Center (Domain 6)	Remarked	Remarked	10%	$5-10\%$	Low	Remarked for mid-energy electrons
Merging Island Reconnection Outflow (Domain 4)	Medium	Not-detected	15%	15%	Relevant for slow electrons	Medium
With Guide Field						
Region	$T_{\parallel}/\mathbf{T}_{\perp_1}$	$T_{\perp_1}/\mathbf{T}_{\perp_2}$	**AO**	$\sqrt{\mathbf{Q}}$	$\mathbf{V}_{\parallel}-\mathbf{V}_{\perp}$	$\theta-\mathbf{V}_{\perp}$
Method Features	Frame-dependent Useful for quick assessments Qualitative results Results similar to both *AO* and $\sqrt{Q}$		Quantitative results *AO* computed in the plane, $\sqrt{Q}$ computed 3D *Relevant disagreement* between the methods in some regions, such as separatrices		Direct Comparison with Satellite observations Direct and Clear Assessment of anisotropy and agyrotropy	
Region X (Domain 1)	Medium	Remarked	5%	15% only on one side	Low	Remarked
Region D (Domain 2)	Remarked	Remarked	15%	15%	Strong double beam flat top distribution	Remarked
Region M (Domain 3)	Remarked	Not-detected	Not-detected	15%	Strong	Not-Detected
Separatrices (Domains 4 and 5)	Medium - Remarked	Remarked	15%	Not-detected	Relevant for slow electrons	Medium
Separatrices (Domains 6)	Medium	Not-detected	$10-15\%$	Not-detected	Relevant for slow electrons	Not-Detected
Plasmoids (Domain 7)	Remarked	Not-detected	$5-10\%$	15%	Remarked	Low for fast electrons

field, we observe a consistent agreement between all the plots, with AO showing quite similar to $\sqrt{Q}$. However, some regions are only highlighted in $T_{\parallel}/T_{\perp_1}$, AO and $\sqrt{Q}$. We explain this effect with the disalignment between the simulation plane and the $\hat{e}_{\perp_1} - \hat{e}_{\perp_2}$ plane. Unlike the case with guide field, where the two planes are almost aligned due to the strong out-of-plane component. However, in this latter case the plots show some remarkable differences. In particular, some regions are especially highlighted in both $T_{\perp_1}/T_{\perp_1}$ and $\sqrt{Q}$, thus denoting regions being both anisotropic and agyrotropic. We interpret this difference as forced by the parallel pressure component entering the $\sqrt{Q}$ equation. The absence of any relevant agyrotropy is confirmed by the phase-spaces in Figure 3, especially in Domains 3 and 7, as well as in Domain 6 with guide field.

References

[1] E. Cazzola, *et al.*, *Phys. Plasmas*, 22(9), 2015.

[2] M.V. Goldman, *et al.*, *Space Science Reviews*, pages 1–38, 2015.

[3] S. Markidis, *et al.*, *Mathematics and Computers in Simulation*, 80(7):1509–1519, 2010.

[4] P.L. Pritchett, *Journal of Geophysical Research: Space Physics (1978–2012)*, 113(A6), 2008.

[5] J. Scudder and W. Daughton, *Journal of Geophysical Research: Space Physics (1978–2012)*, 113(A6), 2008.

[6] M. Swisdak, *Geophysical Research Letters*, 43(1):43–49, 2016. 2015GL066980.

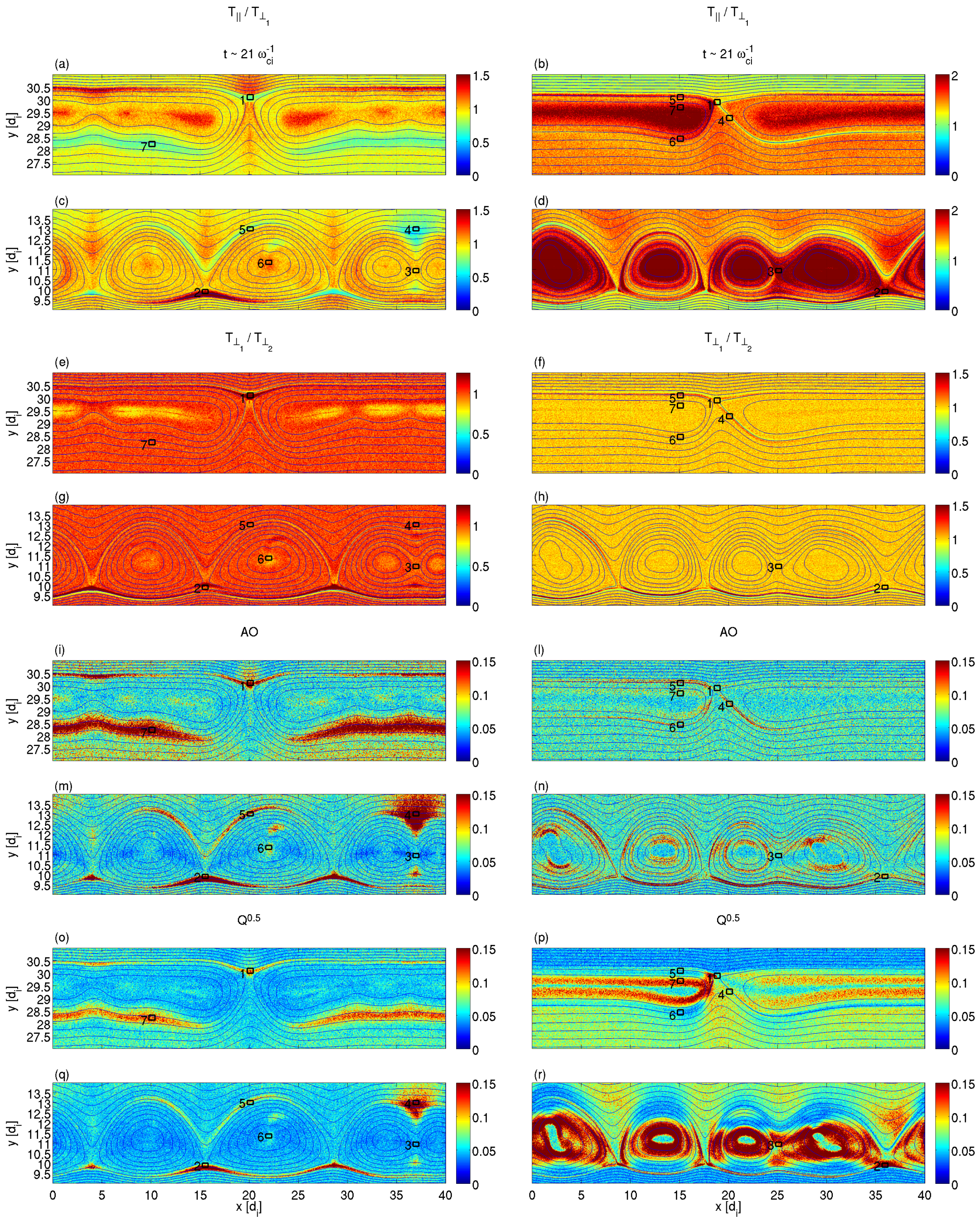

Figure 2: *Plot of $T_{\|}/T_{\perp_1}$, $T_{\perp 1}/T_{\perp_2}$, computed according to [2], AO [5] and $\sqrt{Q}$ [6] for the two current sheets at $t \sim 21\ \omega_{ci}^{-1}$, for the case with no guide field (left panels) and with guide field (right panels). Black boxes indicate the domains considered for the phase-spaces. Domains 1 through 3 represent the X-, D- and M-regions found in [1], while the other domains represent different regions depending on whether with or without guide field.*

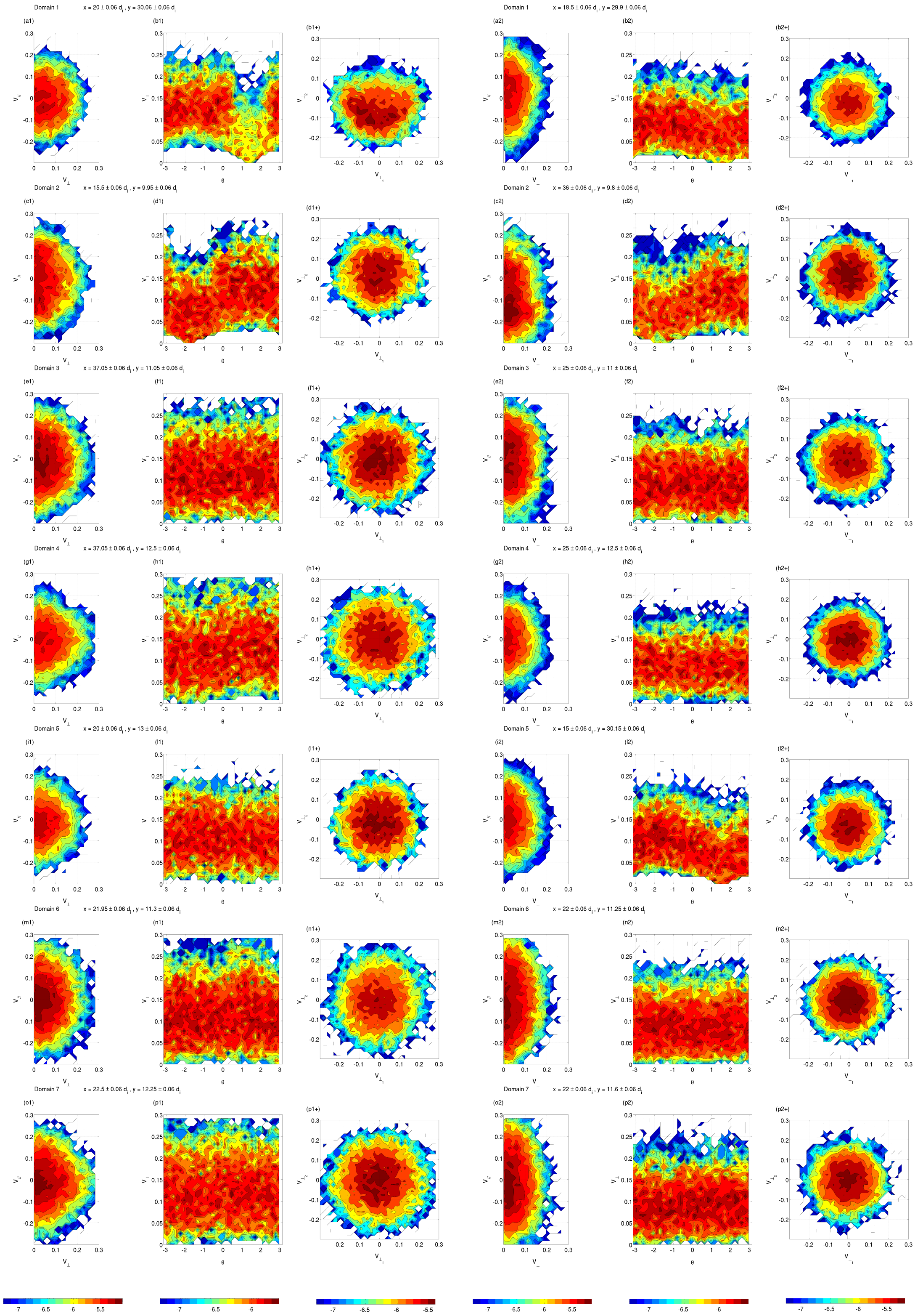

Figure 3: *Set of electron velocity distributions for the domain pointed out with black boxes in figure 2. Color scale indicates the number of particles, in logarithmic scale, over the infinitesimal volume-velocity domain. Panels ending with* 1 *describe the case with no guide field, while those ending with* 2 *the case with guide field. Over the axis* $V_{||}$, $V_{\perp} = \sqrt{V^2 - V_{||}}$ *and* θ. *Finally, panels ending with* + *represent gives a comparison with phase-space in the* $V_{\perp_1} - V_{\perp_2}$ *plane.*